# Weld Pool Shaping and Microstructural Control Using Novel Computer Generated Holographic Optic Laser Welding of Steel and Stainless Steel

R.L.Higginson[1], M.Gibson[2], J.Kell[3], J.Tyrer[2]

[1] Department of Materials, Loughborough University, Loughborough, LE11 3TU, UK

[2] Wolfson School of Mechanical and Manufacturing Engineering, Loughborough University, Loughborough, LE11 3TU, UK.

[3] Now at: Rolls-Royce plc., PO Box 31, Derby, DE24 8BJ

E-mail: R.L.Higginson@lboro.ac.uk

**Keywords:** Laser welding, Holographic Optics, Stainless Steel, Steel, Electron Backscatter Diffraction

**Abstract.** This work considers the use of Holographic Optical Elements (HOEs) to shape the weld beam and control the microstructure of the weld bead. The beam profiles investigated are a standard Gaussian and an Offset Rugby Post produced by a HOE. Autogenous welds have been produced on plain carbon steel with the introduction of a nickel alloy filler powder, using different energy densities. Cross sections of the welds have been analysed in terms of the weld profile, weld pool shape, HAZ and the extent of the deposit/substrate mixing. Electron BackScatter Diffraction (EBSD) coupled with Energy Dispersive X-ray Spectroscopy (EDS) has been used to study the microstructures developed. The results have shown that by utilising HOE's the weld pool shape can be modified so that a squarer profile can be obtained. The grain structure within the weld pool can be controlled such that a finer more equiaxed grain structure can be developed when compared with the coarse columnar grains seen with a Gaussian beam with a marked difference in the microstructures in the HAZ.

## Introduction

Conduction laser welding involves initiating a melt pool by exposure of the metal to high power laser radiation and controlled thermal conduction. A $CO_2$ laser beam, for example, is produced using a gas mix of $CO_2$, $N_2$, and He, which is continually excited by electrodes, to produce a collimated photon beam at 10.6µm. The energy supplied to the metal by this beam is usually sufficient to melt a localised area, usually a joint, with further heating to the surrounding metal within the Heat Affected Zone (HAZ). Traditionally this beam is directed into the work piece using standard optical lenses which produced a circular beam with a Gaussian or other similar energy distribution with little or no scope for controlling the shape of the weld pool, the microstructures within the weld bead or in the HAZ. The energy distribution within a Gaussian beam has the majority of the laser energy at the centre of the beam, with a rapidly decreasing in intensity towards the beam edges. This produces very uneven heating over the interaction region, with the greatest energy absorption at the centre. To provide sufficient heating at the edges of the required region excess heating will be induced at the centre of the weld pool, leading to degradation of resulting microstructures and increased residual stresses. This has been seen when using filler material for repair welding of components [1, 2]

A new way of shaping the beam has been developed at Loughborough University which uses a device called a Holographic Optical Element (HOE). This is effectively a computer generated hologramatic image produced by a small reflecting diffractive mirror comprising of thousands of 6µm squares which are set below the surface at different sub-micron depths [3]. This reflecting optic is placed in the path of the laser beam and the interference and diffraction effect of each element allows the re-shaping of the beam at the reconstructed plane or work piece. The HOE provides a method for shaping the laser beam to tailor the heat profile induced at the material surface, allowing for design of the resulting heat profile present throughout the weld region and

HAZ. A number of studies have been carried out on the use of Holographic optics [4-6], with success demonstrated of the technique in terms of beam control for cutting. To date little work has been carried out on the effect of the microstructural development within the weld however, by using holograms to shape the beam a temperature profile can be designed within the material giving refinement of the weld profile, temperature gradients and microstructural development [7].
Work by the present authors has demonstrated the development of suitable energy distributions to control the weld profile using autogenous weld passes on stainless steel [8]. This work has shown that it is possible to obtain a squarer profile in the weld bead compared to a Gaussian distribution. This is potentially significant for the development of surface cladding using laser welding technologies where the increased volume of material is susceptible to temperature driven weld pool flow, with resulting distortion of the deposition profile. The use of beam shaping in this application allows the manipulation of the weld pool flows to produce a squarer profile allowing the build up of more coherent and homogeneous layers.

**Experimental Procedure**

The substrate material was a 1mm thick low carbon steel sheet with the approximate composition shown in Table 1. Prior to welding the sheets were mechanically cleaned, washed in alcohol and dried. The sheets were laser cut into individual sections to remove heat conduction between deposition regions. The work piece was clamped between two plates of 5 mm mild steel with a 15 mm thick Duratec insulation board beneath the substrate. This arrangement was fixed to the CNC table before tracks of nickel based powder, with the compositions shown in Table 1, were laid across the substrate. The powder was spread in an even layer 0.25mm thick. The laser used was a 1 kW $CO_2$ Coherent Everlase S48 which was fitted either with a coaxial focusing head to produce a Gaussian distribution or a cabinet containing a HOE manufactured to produce an Offset Rugby Post HOE (ORP-HOE) distribution. The relative offset difference on either side of the beam centre was to help determine the influence of the ratio of the height of the edge boundary relative to the centre power level on the metallurgy. A schematic of the energy distributions for the two weld setups are shown in Figure 1. The welds were made using an air assist gas of 10l/min, the role of the gas being to keep spatter and fume from contaminating the laser optics. A number of welds ~30 mm length were completed before the sheet was removed. The Gaussian Deposition was made at 600W and 6mm/s, HOE transverse cross section 600W, 3mm/s to give equivalent welding conditions.

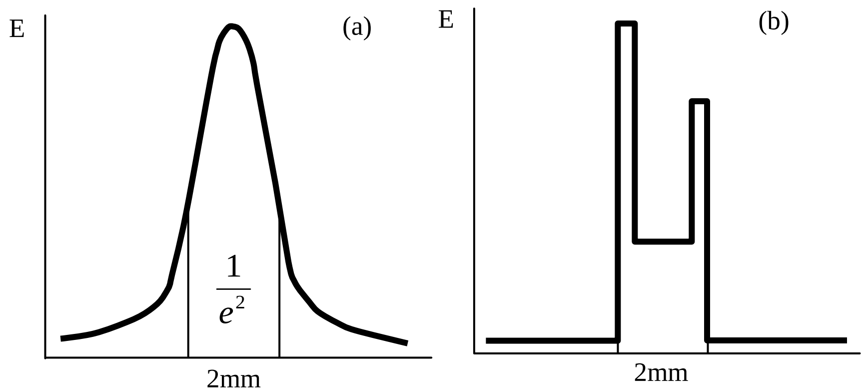


Figure 1: Beam irradiance profiles for (a) Gaussian irradiance distribution and (b) Off Set Rugby Post HOE irradiance distribution.

Following deposition the welds were sectioned both in the transverse and longitudinal directions, mounted in Bakelite and prepared metallographically by grinding and polishing on 6 and 1µm diamond. Prior to examination using electron microscopy the samples were given a final polish using colloidal silica for a minimum of 10 minutes. The samples were examined in a LEO 1530VP Field Emission Gun Scanning Electron Microscope (FEG-SEM) equipped with a TSL-EBSD system with 'Delphi' phase identification and OIM analysis packages. The software allows simultaneous EDS data to be collected during the EBSD scans. Following EBSD examination the samples were etched in 2% Nital to reveal the microstructure of the substrate and optical micrographs taken.

Table 1: Approximate chemical compositions of the mild steel substrate and the nickel based filler powder (wt%)

| | **Fe** | **C** | **Mn** | **P** | **S** | **Ni** | **Cr** | **Co** | **Mo** | **Ti** | **Al** | **Si** | **Nb** | **K** |
|---|---|---|---|---|---|---|---|---|---|---|---|---|---|---|
| Substrate | Bal | 0.15-0.20 | 0.60-0.90 | 0.04 max | 0.05 max | - | - | - | - | - | - | - | - | - |
| Powder | 5max | 0.10 max | 0.50 max | - | 0.015 max | 58 | 20 - 23 | 1.0 max | 8 -10 | 0.40 max | 0.40 max | 0.50 max | 3.15-4.15 | 0.015 max |

## Results and Discussion

Fig.2 shows the optical micrographs of the nickel deposits on mild steel made using a Gaussian Beam and ORP-HOE. The samples were etched to reveal the substrate microstructure. There is a clear difference in the shape of the deposit with that using the Gaussian Beam being more rounded then the ORP-HOE making an average angle of 146° and 135° with the original substrate surface, respectively. There is also a clear difference in the effect of the laser pass on the substrate microstructure. Using the Gaussian Beam the microstructure below the deposit appears to be a primarily Bainite whereas using the ORP-HOE the substrate appears to be a ferrite with areas of Bainite. This indicates there is a difference in both the heat transfer to the substrate as well as a cooling rate.

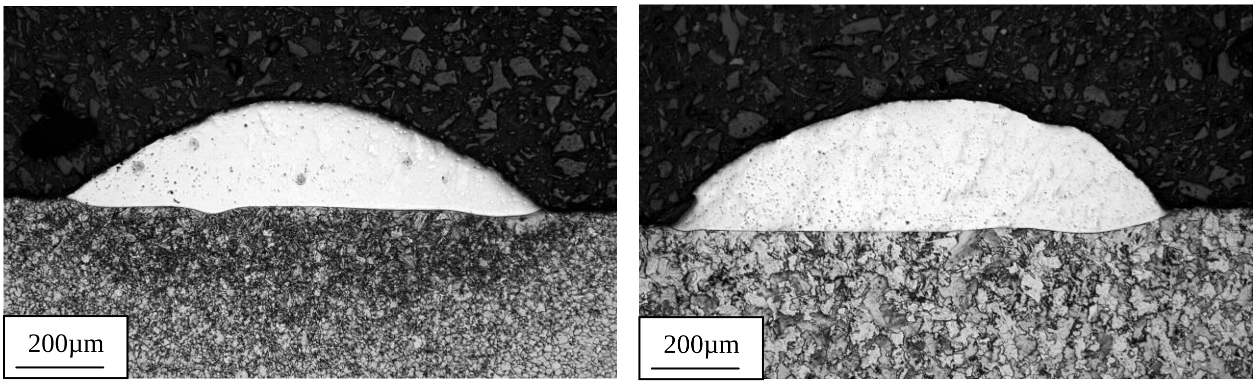


Figure 2: Optical micrographs of (a) the Gaussian Beam and (b) the ORP-HOE deposition of nickel powder onto the mild steel substrate. The samples were etched in 2% Nital to reveal the structure of the substrate.

Fig.3 shows the Inverse Pole Figure (IPF) maps with an overlay of the position of the high angle grain boundaries for the Gaussian and ORP-HOE depositions. The grains in the Gaussian deposition appear to be columnar extending from the substrate out towards the outer edge of the weld bead with a layer of more equiaxed grains on the surface. The substrate again shows how the microstructure is dominated by the Bainitic lath structure. Analysis of the texture of the deposit showed that the grains are randomly orientated. Figure 3(b) shows the EBSD IPF map of the ORP-HOE. The peak of the energy distribution is on the left of the weld. The grains in this deposit are more equiaxed than in Fig.3(a) with a smaller grain size seen on the side with the lower energy input. Again there was no preferred orientation in the grains in the deposit. Fig.4 shows a plot of accumulated grain size for the Gaussian and ORP-HOE deposited material. As seen in Fig.3 there is a clear difference between the grain size on the high and low intensity sides of the HOE so the results are presented both as an average value and separately in Fig.4. The grain diameters of the low and high energy ORP-HOE deposit are ~19μm and 40μm respectively, with the Gaussian deposit ~20μm. There is clearly a grain refinement with the low energy ORP-HOE with a larger grain size seen in the high energy ORP-HOE. These results show that it is possible to control the heat input such that not only can a squarer profile be produced but by controlling the ratio of the peak energy to the distribution width, it should be possible to tailor the grain size to achieve the required mechanical properties.

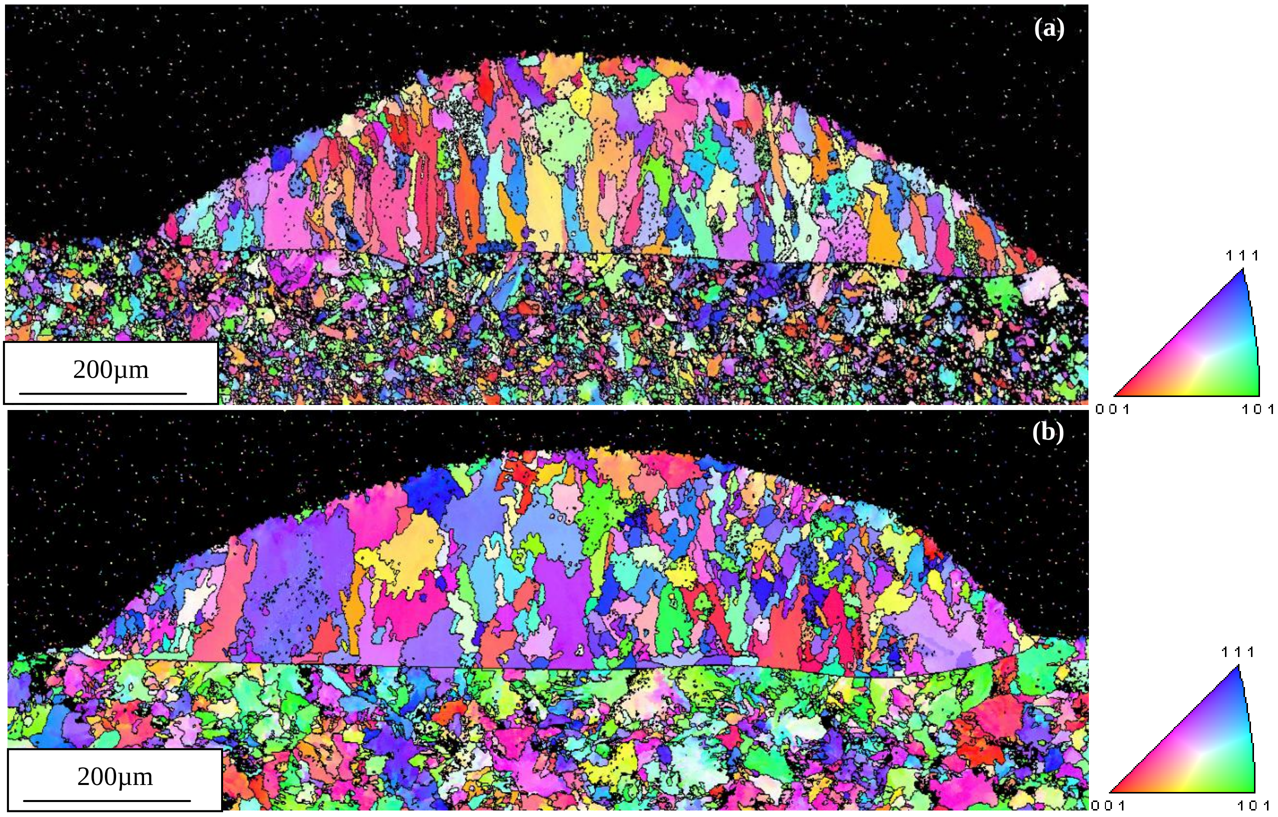


Figure 3: Inverse pole figure and grain boundary map of the deposition of nickel using (a) a standard Gaussian Beam and (b) an ORP- HOE.

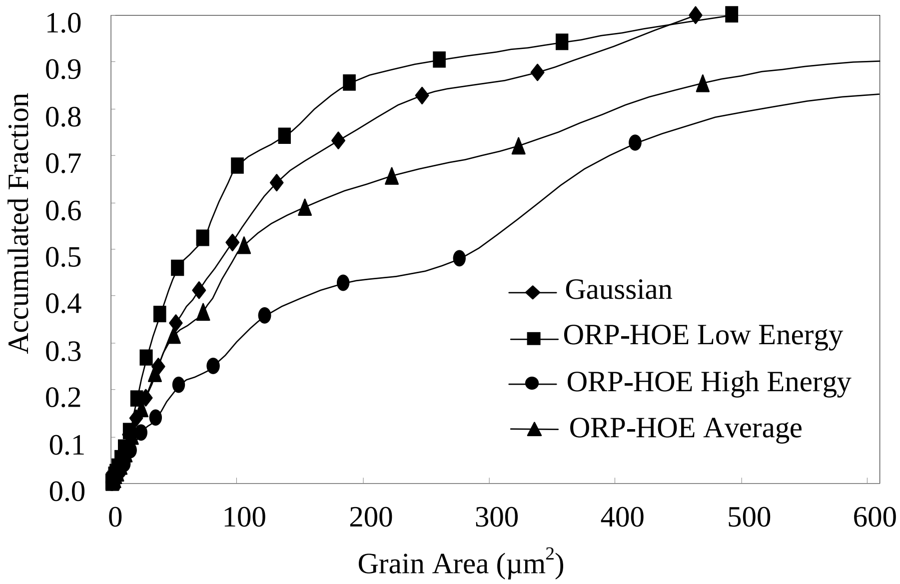


Figure 4: Accumulated grain size plot for the deposited material by Gaussian and ORP-HOE with the high and low energy intensities in the ORP-HOE plotted individually.

Fig.5 shows the Image Quality (IQ) and EDS maps for the nickel and iron for the two deposits. The IQ map shows the microstructure in both the deposit and the substrate. The indexing is better in the deposit than in the substrate showing that there is little lattice strain. In the Substrate below the

Gaussian deposit the IQ is low which corresponds with the Bainite in the HAZ as seen in Fig.2(a). In the HAZ below the ORP-HOE deposit the IQ map is mixed such that a high IQ is seen in the areas of the ferrite and a low IQ in the Bainitic grains giving a mixed microstructure. The EDX maps show that there is little mixing between the deposited material and the substrate using either beam profile. The bottom of the nickel deposit sits below the original substrate surface with only slight mixing seen in the Gaussian beam sample as indicated by the arrows in Fig.5 (c&e).

Fig. 6 shows an IPF map of the ORP-HOE sectioned in the transverse welding direction at approximately the half thickness. At the interface between the substrate and the deposit there is a band of thin grains which are elongated in the beam traverse direction above which are columnar grains which extend towards the surface of the deposit. There is little flow of the microstructure in the beam traverse direction, as indicated by the arrow, which indicates that there is only a slight temperature gradient in the welding direction. The EDX results also showed that there is little mixing between the deposited nickel and the substrate.

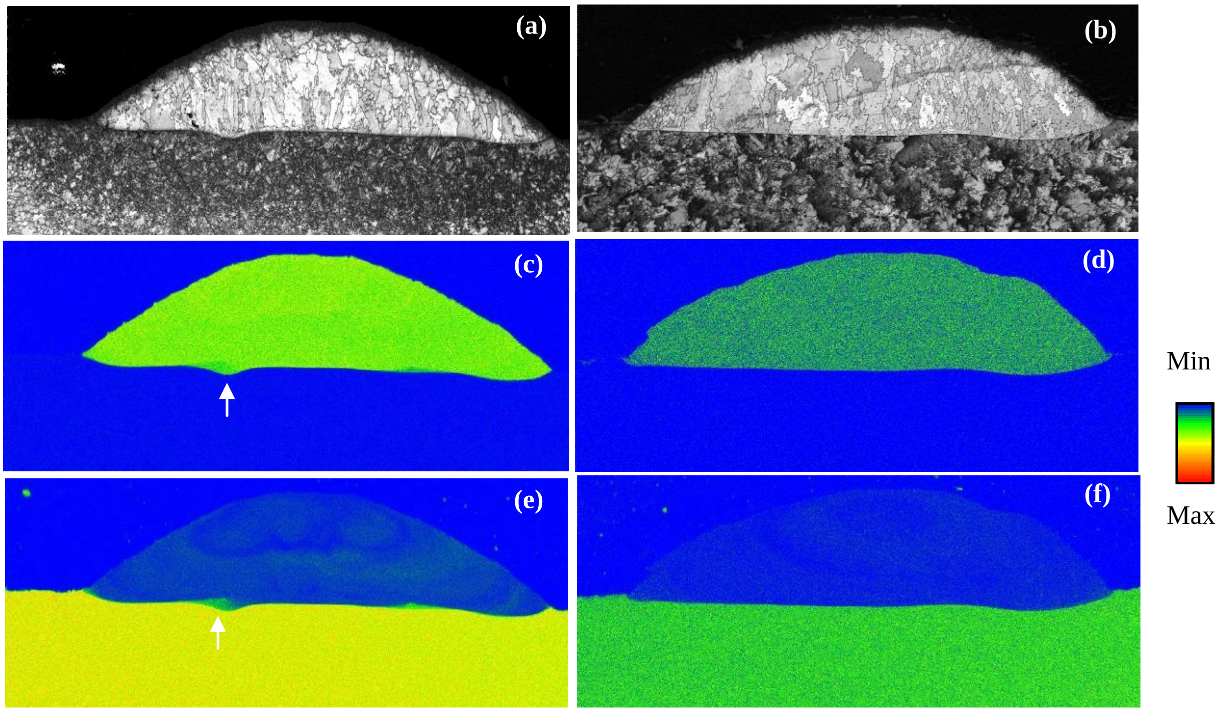


Figure 5: Image quality for (a) the Gaussian and (b) ORP-HOE with corresponding and EDS maps for (c&d) nickel and (e&f) iron.

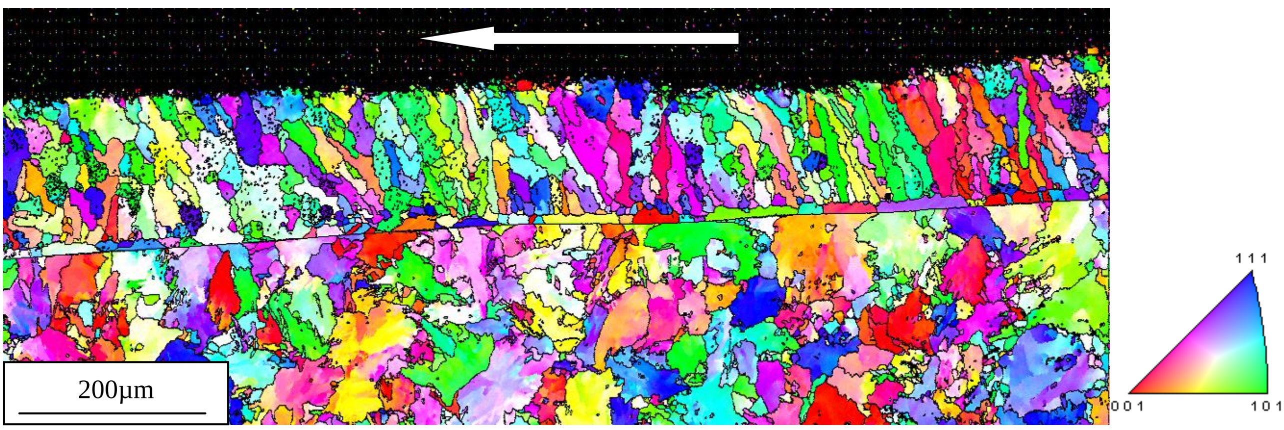


Figure 6: Inverse pole figure map with longitudinal section the deposited nickel using the ORP-HOE. The arrow indicates the direction of the weld traverse.

## Conclusions

Using a Holographic Optic Element (HOE) it is possible to control the energy distribution of the beam. The tailored energy distribution provided by the HOE produces a weld pool with reduced thermal gradients and removal of excessive heating caused by the uneven Gaussian beam. This reduces weld pool flow allowing a squarer bead profile to be established in a deposit which is potentially significant when multi-pass deposits are laid down on a substrate. The grain size within the weld bead/deposit can be controlled such that a finer more equiaxed grain structure can be developed. This grain size control requires the optimisation of the peak energy to beam width ratio such that the energy applied to the material optimises the cooling rate. There is also an advantage in the use of HOEs on the development of the microstructure in the HAZ. With the Gaussian beam the cooling rate is such that Bainite is formed in the substrate below the deposit whereas the HAZ in the HOE deposit is wider and consists of a mixture of ferrite and Bainite. Again there is the potential to control the heat input such that the HAZ can be manipulated to achieve the required cooling rates and hence microstructures. This will have benefits for multi layered deposits so that as the material is built up there is a reduced effect of the weld pass on the underlying material.

## References


[1] P. Bendeich, N. Alam, M. Brandt, D. Carr, K. Short, R. Blevins, *et al.* Mat. Sci. Eng. A Vol. 437(1), (2006;), p. 70

[2] M. Vedani, B. Previtali, G.M. Vimercati, A. Sanvito, G. Somaschini. Surface and Coatings Tech. Vol. 201(8), (2007), p. 4518

[3] S. Noden,. Applications of Diffractive Optical Elements With High Power Lasers. PhD Thesis, Loughborough University, UK, (2000)

[4] S.V. Babin and S.V. Danilov, Optics and Lasers in Eng. Vol. 29 (1998), p.307

[5] K. Fuse, T. Hirai, H. Shiozaki, T. Okada, K. Kurisu, K. Ebata, SEI Tech. Review. Vol.56, (2003), p. 59

[6] M. Ekberg, , M. Larsson, , A. Boller, and S. Hard, Appl. Opt., Vol. 30(25), (1991) p. 3604

[7] M.G. Gibson, J.R. Tyrer, R.L.Higginson, Proc. 27th Int. Congress on Applications of Lasers and Electro-Optics (ICALEO), Temecula, CA, USA, (2008), p. 7

[8] J. Kell, J.R. Tyrer, R.L. Higginson, and R.C. Thomson, Journal of Microscopy, Vol. 2172, (2005), p. 167